



iJRASET

International Journal For Research in
Applied Science and Engineering Technology



INTERNATIONAL JOURNAL FOR RESEARCH

IN APPLIED SCIENCE & ENGINEERING TECHNOLOGY

Volume: 10 **Issue:** XI **Month of publication:** November 2022

DOI: <https://doi.org/10.22214/ijraset.2022.47292>

www.ijraset.com

Call: ☎ 08813907089

E-mail ID: ijraset@gmail.com

Spectral and FTIR Analysis of Tm^{3+} Doped in Zinc Lithium Tungsten Sodalime Borotellurite Glasses

S. L. Meena

Ceramic Laboratory, Department of physics, Jai Narain Vyas University, Jodhpur 342001(Raj) India

Abstract: Glass sample of Zinc Lithium Tungsten Sodalime Borotellurite: $(35-x)\text{TeO}_2:10\text{ZnO}:10\text{Li}_2\text{O}:10\text{WO}_3:10\text{CaO}:10\text{Na}_2\text{O}:15\text{B}_2\text{O}_3:x\text{Tm}_2\text{O}_3$, (where $x=1, 1.5$ and 2 mol%) have been prepared by melt-quenching technique.

The amorphous nature of the prepared glass samples was confirmed by X-ray diffraction. Optical absorption, fluorescence and FTIR spectra were recorded at room temperature for all glass samples. Judd-Ofelt intensity parameters Ω_λ ($\lambda=2, 4$ and 6) are evaluated from the intensities of various absorption bands of optical absorption spectra. Using these intensity parameters various radiative properties like spontaneous emission probability, branching ratio, radiative life time and stimulated emission cross-section of various emission lines have been evaluated

Keywords: ZLTSLBT Glasses, Optical Properties, Judd-Ofelt Theory, Rare earth ions.

I. INTRODUCTION

Transparent glass-ceramic as host materials for active optical ions have attracted great interest recently due to their potential application in optical devices such as frequency-conversion materials, lasers and optical fiber amplifiers [1-5]. Among these hosts, the borotellurite system is attractive due to its superior physical, structural and optical properties [6, 7]. ZnO is a wide band gap semiconductor and has received increasing research interest. It is an important multifunctional material due to its specific chemical, surface and micro structural properties [8]. Tellurite glasses have a low glass transition temperature, low melting temperature and high gain density.

The high gain density in tellurite glasses is due to high solubility of rare earth ions in tellurite network [9-14]. Recently, glass-ceramics containing dysprosium oxides have been found in applications for several different purposes. Tm^{3+} doped glasses have attracted much interest due to their important optical properties used in lasers, optical amplifiers, network formers, photonic devices and as infrared sensors [15-18].

The present work reports on the preparation and characterization of rare earth doped heavy metal oxide (HMO) glass systems for lasing materials. I have studied on the absorption, emission and FTIR properties of Tm^{3+} doped zinc lithium tungsten sodalime borotellurite glasses.

The intensities of the transitions for the rare earth ions have been estimated successfully using the Judd-Ofelt theory, The laser parameters such as radiative probabilities(A), branching ratio (β), radiative life time(τ_R) and stimulated emission cross section(σ_p) are evaluated using J.O.intensity parameters(Ω_λ , $\lambda=2, 4$ and 6).

II. EXPERIMENTAL TECHNIQUES

A. Preparation of Glasses

The following Tm^{3+} doped borotellurite glass samples $(35-x)\text{TeO}_2:10\text{ZnO}:10\text{Li}_2\text{O}:10\text{WO}_3:10\text{CaO}:10\text{Na}_2\text{O}:15\text{B}_2\text{O}_3:x\text{Tm}_2\text{O}_3$, (where $x=1, 1.5$ and 2 mol%) have been prepared by melt-quenching method. Analytical reagent grade chemical used in the present study consist of TeO_2 , ZnO, Li_2O , WO_3 , CaO, Na_2O , B_2O_3 and Tm_2O_3 .

They were thoroughly mixed by using an agate pestle mortar. then melted at 980°C by an electrical muffle furnace for 2h., After complete melting, the melts were quickly poured in to a preheated stainless steel mould and annealed at temperature of 250°C for 2h to remove thermal strains and stresses. Every time fine powder of cerium oxide was used for polishing the samples. The glass samples so prepared were of good optical quality and were transparent. The chemical compositions of the glasses with the name of samples are summarized in Table 1.

Table 1.

Chemical composition of the glasses

Sample	Glass composition (mol %)
ZLTSLBT (UD)	35TeO ₂ :10ZnO:10Li ₂ O:10WO ₃ :10CaO:10Na ₂ O:15B ₂ O ₃
ZLTSLBT (TM1)	34TeO ₂ :10ZnO:10Li ₂ O:10WO ₃ :10CaO:10Na ₂ O:15B ₂ O ₃ :1Tm ₂ O ₃
ZLTSLBT (TM1.5)	33.5TeO ₂ :10ZnO:10Li ₂ O:10WO ₃ :10CaO:10Na ₂ O:15B ₂ O ₃ :1.5Tm ₂ O ₃
ZLTSLBT (TM 2)	33TeO ₂ :10ZnO:10Li ₂ O:10WO ₃ :10CaO:10Na ₂ O:15B ₂ O ₃ :2 Tm ₂ O ₃

ZLTSLBT (UD) -Represents undoped Zinc Lithium Tungsten Sodalime Borotellurite glass specimen.

ZLTSLBT (TM) -Represents Tm³⁺ doped Zinc Lithium Tungsten Sodalime Borotellurite glass specimens.

III. THEORY

A. Oscillator Strength

The intensity of spectral lines are expressed in terms of oscillator strengths using the relation [19].

$$f_{\text{expt.}} = 4.318 \times 10^{-9} [\epsilon(\nu) d \nu] \quad (1)$$

where, $\epsilon(\nu)$ is molar absorption coefficient at a given energy ν (cm⁻¹), to be evaluated from Beer–Lambert law.

Under Gaussian Approximation, using Beer–Lambert law, the observed oscillator strengths of the absorption bands have been experimentally calculated [20], using the modified relation:

$$P_m = 4.6 \times 10^{-9} \times \frac{1}{cl} \log \frac{I_0}{I} \times \Delta\nu_{1/2} \quad (2)$$

where c is the molar concentration of the absorbing ion per unit volume, l is the optical path length, $\log I_0/I$ is optical density and $\Delta\nu_{1/2}$ is half band width.

B. Judd-Ofelt Intensity Parameters

According to Judd [21] and Ofelt [22] theory, independently derived expression for the oscillator strength of the induced forced electric dipole transitions between an initial J manifold $|4f^N(S, L) J\rangle$ level and the terminal J' manifold $|4f^N(S', L') J'\rangle$ is given by:

$$\frac{8\pi^2 mc \bar{\nu}}{3h(2J+1)n} \left[\frac{(n^2+2)^2}{9} \right] \times S(J, J') \quad \text{Where,} \quad (3)$$

the line strength $S(J, J')$ is given by the equation

$$S(S', L') = e^2 \sum_{\lambda=2,4,6} \Omega_{\lambda} \langle 4f^N(S, L) J \| U^{(\lambda)} \| 4f^N(S', L') J' \rangle^2 \quad (4)$$

In the above equation m is the mass of an electron, c is the velocity of light, $\bar{\nu}$ is the wave number of the transition, h is Planck's constant, n is the refractive index, J and J' are the total angular momentum of the initial and final level respectively, Ω_{λ} ($\lambda=2,4$ and 6) are known as Judd-Ofelt intensity parameters.

C. Radiative Properties

The Ω_{λ} parameters obtained using the absorption spectral results have been used to predict radiative properties such as spontaneous emission probability (A) and radiative life time (τ_R), and laser parameters like fluorescence branching ratio (β_R) and stimulated emission cross section (σ_p).

The spontaneous emission probability from initial manifold $|4f^N(S', L') J'\rangle$ to a final manifold $|4f^N(S, L) J\rangle$ is given by:

$$A[(S', L') J'; (S, L) J] = \frac{64 \pi^2 \bar{\nu}^3}{3h(2J'+1)} \left[\frac{n(n^2+2)^2}{9} \right] \times S(J', J) \quad (5)$$

Where, $S(J', J) = e^2 [\Omega_2 \| U^{(2)} \|^2 + \Omega_4 \| U^{(4)} \|^2 + \Omega_6 \| U^{(6)} \|^2]$

The fluorescence branching ratio for the transitions originating from a specific initial manifold $|4f^N(S', L') J' \rangle$ to a final many fold $|4f^N(S, L) J \rangle$ is given by

$$\beta[(S', L') J'; (S, L) J] = \frac{A[(S', L') J'; (S, L) J]}{\sum_{S, L, J} A[(S', L') J'; (S, L) J]} \quad (6)$$

where, the sum is over all terminal manifolds.

The radiative life time is given by

$$\tau_{rad} = \frac{1}{\sum_{S, L, J} A[(S', L') J'; (S, L) J]} = A_{Total}^{-1} \quad (7)$$

where, the sum is over all possible terminal manifolds. The stimulated emission cross-section for a transition from an initial manifold $|4f^N(S', L') J' \rangle$ to a final manifold $|4f^N(S, L) J \rangle$ is expressed as

$$\sigma_p(\lambda_p) = \left[\frac{\lambda_p^4}{8\pi c n^2 \Delta\lambda_{eff}} \right] \times A[(S', L') J'; (S, L) J] \quad (8)$$

where, λ_p the peak fluorescence wavelength of the emission band and $\Delta\lambda_{eff}$ is the effective fluorescence line width.

IV. RESULT AND DISCUSSION

A. XRD Measurement

Figure 1 presents the XRD pattern of the sample contain – TeO_2 which is show no sharp Bragg's peak, but only a broad diffuse hump around low angle region. This is the clear indication of amorphous nature within the resolution limit of XRD instrument

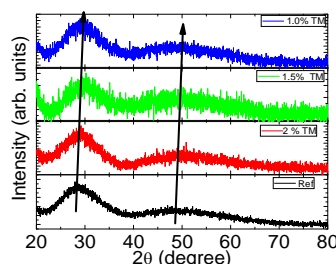


Fig. 1 X-ray diffraction pattern of $\text{TeO}_2\text{:ZnO:Li}_2\text{O:WO}_3\text{:CaO:Na}_2\text{O:B}_2\text{O}_3\text{: Tm}_2\text{O}_3$.

B. FTIR Transmission Spectrum

The FTIR spectrum of ZLTSLBT TM (01) glass is in the wave number range $400\text{--}1600\text{ cm}^{-1}$ is presented in Fig.2 and the possible mechanism bands are tabulated in Table 2.

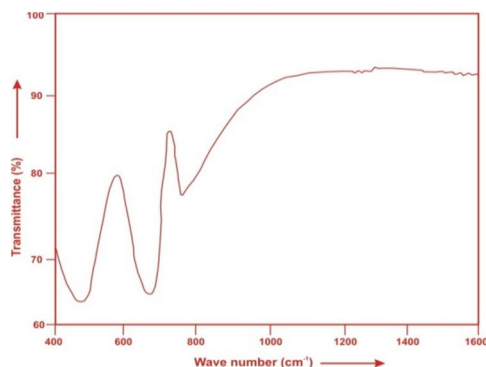


Fig. (2) FTIR spectrum of ZLTSLBT TM (01) glass.

In the studied glasses, the absorption band at 426 cm^{-1} is appeared due to the symmetric stretching vibration of the Zn-O bond [23].whereas the band at 680 cm^{-1} is due to the stretching vibrations of Te-O bonds in trigonal bipyramidal units TeO_4 (tbp) [24]. The band at 771 cm^{-1} is evolved for pure and doped glasses due to trigonal pyramidal structural units. This band is attributed to the stretching vibration within the tellurium and the non-bridging oxygen of trigonal pyramidal structure [25].

Table2. Assignment of infrared transmission bands of (ZLTSLBT TM 01) glass.

Peak position(cm^{-1})	Band Assignment
~ 465	symmetric stretching vibration of the Zn-O bond [23]
~ 680	stretching vibrations of Te-O bonds in trigonal bipyramidal units TeO_4 [24]
~ 771	trigonal pyramidal structural units [25]

C. Absorption Spectrum

The absorption spectra of Tm^{3+} doped ZLTSLBT glass specimens have been presented in Figure 3 in terms of optical density versus wavelength. Five absorption bands have been observed from the ground state $^3\text{H}_6$ to excited states $^3\text{F}_4$, $^3\text{H}_5$, $^3\text{H}_4$, $^3\text{F}_3$ and $^1\text{G}_4$ for Tm^{3+} doped ZLTSLBT glasses.

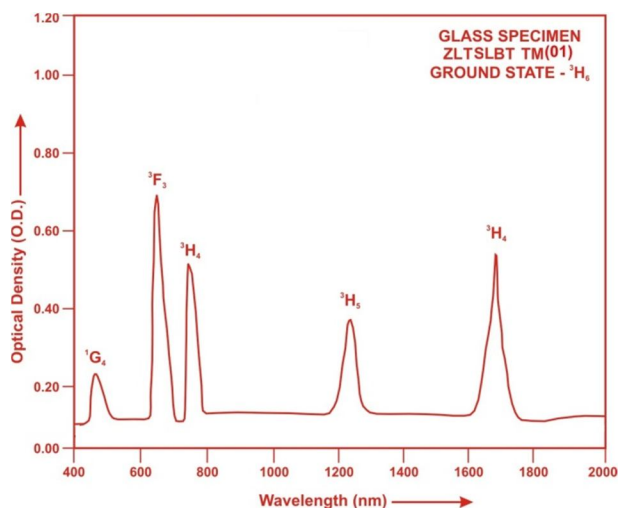


Fig. (3) Absorption spectrum of ZLTSLBT TM (01) glass.

The experimental and calculated oscillator strength for Tm^{3+} ions in ZLTSLBT glasses are given in Table 3.

Table 3: Measured and calculated oscillator strength ($P_m \times 10^{+6}$) of Tm^{3+} ions in ZLTSLBT glasses.

Energy level from $^3\text{H}_6$	Glass ZLTSLBT (TM01)		Glass ZLTSLBT (TM1.5)		Glass ZLTSLBT (TM02)	
	$P_{\text{exp.}}$	$P_{\text{cal.}}$	$P_{\text{exp.}}$	$P_{\text{cal.}}$	$P_{\text{exp.}}$	$P_{\text{cal.}}$
$^3\text{F}_4$	1.80	1.85	1.77	1.83	1.74	1.81
$^3\text{H}_5$	1.36	1.45	1.32	1.44	1.30	1.43
$^3\text{H}_4$	1.96	2.06	1.93	2.05	1.90	2.04
$^3\text{F}_3$	2.92	3.03	2.89	3.02	2.84	2.99
$^1\text{G}_4$	0.71	0.89	0.67	0.89	0.63	0.89
r.m.s. deviation	± 0.11663		± 0.14050		± 0.16291	

In the Zinc Lithium Tungsten Sodalime Borotellurite glasses (ZLTSLBT) Ω_2 , Ω_4 and Ω_6 parameters decrease with the increase of x from 1 to 2 mol%. The order of magnitude of Judd-Ofelt intensity parameters is $\Omega_4 > \Omega_2 > \Omega_6$ for all the glass specimens. The spectroscopic quality factor (Ω_4 / Ω_6) related with the rigidity of the glass system has been found to lie between 1.401 and 1.439 in the present glasses.

The values of Judd-Ofelt intensity parameters are given in Table 4.

Table 4: Judd-Ofelt intensity parameters for Tm^{3+} doped ZLTSLBT glass specimens

Glass Specimen	$\Omega_2(\text{pm}^2)$	$\Omega_4(\text{pm}^2)$	$\Omega_6(\text{pm}^2)$	Ω_4/Ω_6
ZLTSLBT (TM 01)	6.367	7.733	5.373	1.439
ZLTSLBT (TM 1.5)	6.276	7.649	5.359	1.427
ZLTSLBT (TM 02)	6.268	7.489	5.347	1.401

D. Fluorescence Spectrum

The fluorescence spectrum of Tm^{3+} doped in glass is shown in Figure 4. There are nine broad bands observed in the Fluorescence spectrum of Tm^{3+} doped zinc lithium tungsten sodalime borotellurite glass. The wavelengths of these bands along with their assignments are given in Table 5. The peak with maximum emission intensity appears at 1810 nm and corresponds to the ($^3\text{F}_4 \rightarrow ^3\text{H}_6$) transition.

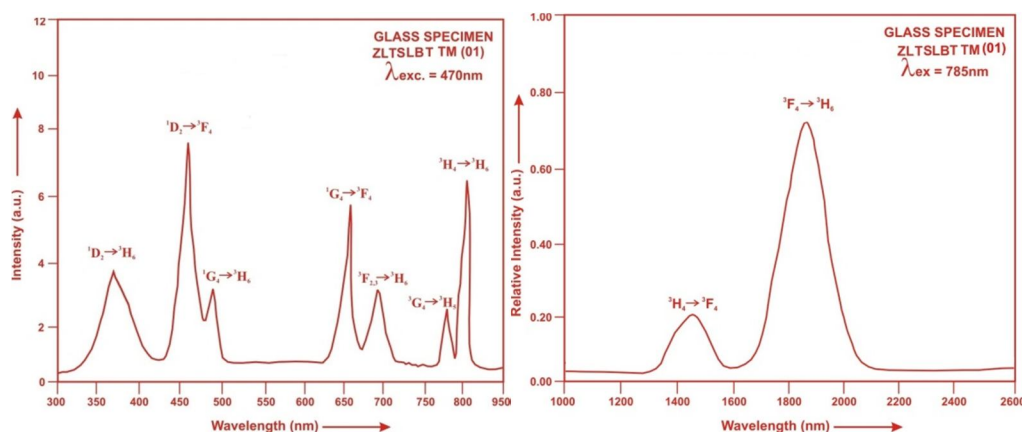


Fig. (4). Fluorescence spectrum of ZLTSLBT TM (01) glass.

Table 5: Emission peak wave lengths (λ_p), radiative transition probability (A_{rad}), branching ratio (β), stimulated emission cross-section (σ_p) and radiative life time (τ_R) for various transitions in Tm^{3+} doped ZLTSLBT glasses

Transition	λ_{max} (nm)	ZLTSLBT (TM 01)				ZLTSLBT (TM 1.5)				ZLTSLBT (TM 02)			
		$A_{\text{rad}}(\text{s}^{-1})$	β	σ_p (10^{-20} cm^2)	$\tau_R(\mu\text{s})$	$A_{\text{rad}}(\text{s}^{-1})$	β	σ_p (10^{-20} cm^2)	$\tau_R(\mu\text{s})$	$A_{\text{rad}}(\text{s}^{-1})$	β	σ_p (10^{-20} cm^2)	τ_R (10^{-20} cm^2)
$^1\text{D}_2 \rightarrow ^3\text{H}_6$	365	59863.50	0.6277	1.482	10.4853	59484.40	0.6281	1.516	10.5594	58663.10	0.6258	1.558	10.668
$^1\text{D}_2 \rightarrow ^3\text{F}_4$	455	19680.30	0.2064	2.302		19466.80	0.2056	2.462		19416.00	0.2071	2.656	
$^1\text{G}_4 \rightarrow ^3\text{H}_6$	480	2476.11	0.0259	0.548		2452.76	0.0259	0.576		2425.11	0.0259	0.628	
$^1\text{G}_4 \rightarrow ^3\text{F}_4$	651	812.57	0.0085	1.478		809.74	0.0086	1.627		805.60	0.0086	2.362	
$^3\text{F}_{2,3} \rightarrow ^3\text{H}_6$	689	6143.18	0.0644	2.309		6121.39	0.0646	2.422		6080.14	0.0648	2.485	
$^1\text{G}_4 \rightarrow ^3\text{H}_5$	785	2369.10	0.0248	2.453		2363.50	0.0250	2.630		2361.71	0.0252	2.800	
$^3\text{H}_4 \rightarrow ^3\text{H}_6$	798	3128.37	0.0328	4.319		3112.41	0.0329	4.748		3104.71	0.0331	5.239	
$^3\text{H}_4 \rightarrow ^3\text{F}_4$	1450	398.35	0.0042	3.745		395.66	0.0042	3.831		393.13	0.0042	3.987	
$^3\text{F}_4 \rightarrow ^3\text{H}_6$	1810	500.30	0.0052	7.138		495.77	0.0052	7.200		490.79	0.0052	7.306	

V. CONCLUSION

In the present study, the glass samples of composition $(35-x)\text{TeO}_2:10\text{ZnO}:10\text{Li}_2\text{O}:10\text{WO}_3:10\text{CaO}:10\text{Na}_2\text{O}:15\text{B}_2\text{O}_3:x\text{Tm}_2\text{O}_3$, (where $x = 1, 1.5$ and $2\text{mol } \%$) have been prepared by melt-quenching method. The value of stimulated emission cross-section (σ_p) is found to be maximum for the transition ($^3\text{F}_4 \rightarrow ^3\text{H}_6$) for glass ZLTSLBT (TM 01), suggesting that glass ZLTSLBT (TM 01) is better compared to the other two glass systems ZLTSLBT (TM 1.5) and ZLTSLBT (TM 02).

REFERENCES

- [1] Zhang ,X.,Hu,L. and Ren,J. (2020). Structural Studies of Rare Earth-Doped Fluoroborosilicate Glasses by Advanced Solid-State NMR, . Phys.Chem.123(16),8919-8929.
- [2] Liyu Hao, Manting Pei, Tie Yang, Chengguo Ming(2020).Double sensitivity temperature sensor based on excitation intensity ratio of Eu^{3+} doped phosphate glass ceramic, Optik 204,164188.
- [3] Areej, S. Alqarni, R., Hussin, S.N., Alamri and Ghoshal, S.K.(2020).Tailored structures and dielectric traits of holmium ion-doped zinc-sulpho-boro-phosphate glass ceramics, Ceramics International 46(3),3282-3291.
- [4] Haijian Li, Jianhua Yi, Zhao Qin, Zhihua Sun, Yi Xu, Changjian Wang, Fengqi Zhao, Yucheng Hao and Xiaofeng L., (2019). Structures, Thermal expansion, chemical stability and crystallization behavior of phosphate based glasses by influence of rare earth, Journal of Non- Crystalline Solids 522,119602.
- [5] Mikko Hongisto, Alexander Vebar, Nadia Giovanna, S. Danto, Veronique and L. Petit(2020).Transparent Yb^{3+} doped phosphate glass ceramics, Ceramics International 46(16),26317-26325.
- [6] Elkhoshkhany,N., Khatib, M.A. and Kabary, M.A.(2018).Thermal, FTIR and UV spectral studies on tellurite glasses doped with cerium oxide,Ceram Int, 44 , 2789-2796.
- [7] Wagh, A., Raviprakash,Y., Upadhyaya, V. and Kamath, S.D.(2015).Composition dependent structural and optical properties of $\text{PbF}_2\text{-TeO}_2\text{-B}_2\text{O}_3\text{-Eu}_2\text{O}_3$ glasses, Spectrochim Acta A Mol Biomol Spectrosc, 151, 696-706
- [8] Pavani, P. G., Sadhana, K. and Mouli, V. C. (2011).Optical, physical and structural studies of boro-zinc tellurite glasses, Physica B: Condensed Matter, 406, 7, 1247.
- [9] P.Nandi and G.Jose (2006). Spectroscopic Properties of Er^{3+} Doped Phospho-Tellurite Glasses,Physica B Condensed Matter,381(1),66-72.
- [10] Anashkina, E.A.(2020).Laser Sources Based on Rare-Earth Ion Doped Tellurite Glass Fibers and Microspheres, Fibers , 8,1-17.
- [11] Jha, A., Richards, B., Jose, G., Teddy-Fernandez, T., Joshi, P.m, Jiang, X. and Lousteau(2012).J. Rare-earth ion doped TeO_2 and GeO_2 glasses as laser materials. Prog. Mater. Sci., 57, 1426-1491
- [12] Kishi, T., Kumagai, T., Shibuya, S., Prudenzeno, F., Yano, T. and Shibata, S.(2015). Quasi-single mode laser output from a terrace structure added on Nd^{3+} -doped tellurite-glass microsphere prepared using localized laser heating. Opt. Express, 23, 20629-20635.
- [13] Anashkina, E. A.(2020). Laser Sources Based on Rare-Earth Ion Doped Tellurite Glass Fibers and Microspheres, Fibers , 8 (30),1-17.
- [14] Qin, J., Huang, Y., Liao, T., Xu, C., Ke, C. and Duan, Y.(2019). 1.9 μm laser and visible light emissions in $\text{Er}^{3+}/\text{Tm}^{3+}$ co-doped tellurite glass microspheres pumped by a broadband amplified spontaneous emission source. J. Opt., 21, 035401.
- [15] Lachheb, R., Damak, K., Assadi, A.A., Herrmann, A., Yousef, E., Rüssel, C.and Maâlej, R.(2015). Characterization of Tm^{3+} doped TNZL glass laser material. J. Lumin., 161, 281-287.
- [16] Lalla, E.A., Konstantinidis, M., De Souza, I., Daly, M.G., Martín, I.R., Lavín, V. and Rodríguez-Mendoza, U.R.(2020). Judd-Ofelt parameters of RE^{3+} -doped fluorotellurite glass ($\text{RE}^{3+} = \text{Pr}^{3+}, \text{Nd}^{3+}, \text{Sm}^{3+}, \text{Tb}^{3+}, \text{Dy}^{3+}, \text{Ho}^{3+}, \text{Er}^{3+}$, and Tm^{3+}). J. Alloys Compd., 845, 156028.
- [17] El-Maaref, A.A., Wahab, E. A., Shaaban, Kh S., Abdelawwad, M., Koubisy, M. S., Boercsoek, J.and Sayed Yousef, El (2020).Visible and mid-infrared spectral emissions and radiative rates calculations of Tm^{3+} doped BBLC glass, Spectrochimica Acta Part A- Molecular and Biomolecular Spectroscopy, 242, 118774.
- [18] Sharma, R., Prasad, A., Kaur, S., Deopa,N., Rani, R., Venkateswarlu, M.and Rao, A.S.(2019). Spectroscopic properties of deep red emitting Tm^{3+} doped ZnPbWTe glasses for optoelectronic and laser applications, Journal of NonCrystalline Solids. 516, 82-88.
- [19] Gorller-Walrand, C. and Binnemans, K. (1988). Spectral Intensities of f-f Transition. In: Gshneidner Jr., K.A. and Eyring, L., Eds., Handbook on the Physics and Chemistry of Rare Earths, Vol. 25, Chap. 167, North-Holland, Amsterdam, 101.
- [20] Sharma, Y.K., Surana, S.S.L. and Singh, R.K. (2009). Spectroscopic Investigations and Luminescence Spectra of Sm^{3+} Doped Soda Lime Silicate Glasses. Journal of Rare Earths, 27, 773.
- [21] Judd, B.R. (1962). Optical Absorption Intensities of Rare Earth Ions. Physical Review, 127, 750.
- [22] Ofelt, G.S. (1962). Intensities of Crystal Spectra of Rare Earth Ions. The Journal of Chemical Physics, 37, 511.
- [23] Elkhoshkhany,N., Marzouk, S. Y., Khattab, M. A.and Dessouki, S. A.(2018). Influence of Sm_2O_3 addition on JuddOfelt parameters, thermal and optical properties of the $\text{TeO}_2\text{-Li}_2\text{O-ZnO-Nb}_2\text{O}_5$ glass system, Mater. Charact. 144 274-286.
- [24] Elkhoshkhany, N.and Mohamed, H.M.(2019). UV-Vis-NIR spectroscopy, structural and thermal properties of novel oxyhalide tellurite glasses with composition $\text{TeO}_2\text{-B}_2\text{O}_3\text{-SrCl}_2\text{-LiF-Bi}_2\text{O}_3$ for optical application. Res. Phys., 13, 102222.
- [25] Mansour, E.(2012). FTIR spectra of pseudo-binary sodium borate glasses containing TeO_2 , J. Mol. Struct. 1014, 1-6.



10.22214/IJRASET



45.98



IMPACT FACTOR:
7.129



IMPACT FACTOR:
7.429



INTERNATIONAL JOURNAL FOR RESEARCH

IN APPLIED SCIENCE & ENGINEERING TECHNOLOGY

Call : 08813907089  (24*7 Support on Whatsapp)